

# ANNALS of Faculty Engineering Hunedoara – International Journal of Engineering

Tome XIV [2016] – Fascicule 2 [May]

ISSN: 1584-2665 [print; online]

ISSN: 1584-2673 [CD-Rom; online]

a free-access multidisciplinary publication  
of the Faculty of Engineering Hunedoara



<sup>1</sup>. I.I. AHMED, <sup>2</sup>. J.A. ADEBISI, <sup>3</sup>. T. YAHAYA,  
<sup>4</sup>. N.I. AREMU, <sup>5</sup>. A.H. SHERRY

## ASSESSMENT OF CRACK PROPAGATION MODE IN MARTENSITIC STAINLESS STEEL HAZ WITH ELECTRON BACK SCATTER DIFFRACTION: EFFECTS OF ENVIRONMENTAL VARIABLES

<sup>1,5</sup>. Materials Performance Centre, University of Manchester, Manchester, M13 9PL, UNITED KINGDOM

<sup>2-4</sup>. Department of Materials and Metallurgical Engineering, University of Ilorin, Ilorin, NIGERIA

**ABSTRACT:** In this study, an assessment of crack propagation mode in martensitic stainless steels heat affected zone was carried out with electron back scatter diffraction (EBSD) with focus on the effect of environmental variables. Girth welded samples were subjected to four point bend tests in sour and sweet environments. Scanning electron microscope and electron back scatter diffraction technique were both used to study the crack propagation mode and interaction of crack tip with microstructures. Study showed that sample tested in sour environment failed with transgranular cracking and samples tested in sweet environment failed with intergranular stress corrosion cracking mode. The proposed mechanism for the failure was sulphide stress corrosion cracking and intergranular precipitation of carbide by sensitisation process respectively. The correlation between crack path and grains misorientation was studied with aid of EBSD technique.

**Keywords:** crack; corrosion environment; EBSD; HAZ; martensitic; weld

### 1. INTRODUCTION

The high carbon grades of martensitic stainless steels (MSS) have a number of challenges including weldability and susceptibility to stress corrosion cracking (SCC) attributed to sensitisation. Its heat affected zone (HAZ) suffers from cracks attributed to high hardness (Griffiths et al., 2004, Coudreuse et al., 1999). However, attempted use of low carbon grades with carbon contents less than 0.02%C to mollify the SCC susceptibility was not without challenge either. Their deployment as down hole tubular for oil and gas transportations in sweet (H<sub>2</sub>S free) and sour environments (Enerhaug and Steinsmo, 2001, Kurahashi et al., 1985) required joining and fabrication including welding. Though, the low C content enables the steels to be welded without preheating and post weld heat treatment (PWHT) (Turnbull and Griffiths, 2003), in addition to reduced susceptibility to SCC (Griffiths et al., 2004), but the effects of metallurgical alteration of the fusion boundary and neighbouring HAZ due to weld metal dilution and elemental diffusion needed attention to properly address the challenge of SCC.

Stress corrosion cracking is caused by the action of mechanical (including residual) stresses on susceptible materials in aggressive environments (Hanneman et al., 1979, Williams et al., 1979, National Energy Board, 1996, Ahmed et al., 2014a). Welded joints are quite vulnerable to cracking depending on the service environment and the presence of internal stresses (Messler, 2008, Aquino et al., 2009). This study looks at the cracking mechanism of MSS in sour and sweet environments with focus on the effects of environmental variables. Scanning electron microscope and electron back scatter diffraction method were both used for assessment of crack propagation mode.

## 2. EXPERIMENTAL PROCEDURE

### 2.1. Materials

The materials used for the study was low carbon martensitic stainless steels. The materials were provided by the welding institute, (TWI) Cambridge, United Kingdom. The original MSS pipe without any welding heat input is referred to as the parent steel and the weld metal is actual joint fabricated with filler wire. The detail chemical compositions of the parent, weld and filler metals are shown in Table 1. The description of the welding process used for the fabrication of MSS pipes is given below.

**Table 1:** Chemical composition of the specimens used for experimentation (parent material and weld metal) and the filler wire used

Description	Elements (weight percent, wt %)									
	C	N	Si	Mn	P	Ti	Cr	Mo	Ni	Al
Parent steels	0.009	0.005	0.20	0.43	0.014	0.120	12.20	2.51	6.40	0.03
Weld metal	0.019	0.185	0.34	0.40	0.017	0.026	22.00	3.58	8.50	0.02
Filler (1.2mm $\phi$ )	0.027	0.232	0.40	0.41	0.016	NA	26.10	3.90	9.30	NA

### 2.2. Welding of MSS Pipes

Mechanised pulsed gas metal Arc (PGMA) welding process was used for the fabrication of the MSS pipes at TWI, Cambridge. The PGMA welding process is notable for significantly lower welding porosity. The Gas metal arc welding process used 1.2 mm diameter superduplex stainless steel (detailed composition in Table 1) as continuous filler wire electrode and an externally supplied inert shielding gases comprising Ar/He/CO<sub>2</sub>/N<sub>2</sub>. The consumable wire electrode produced an arc with the work piece which formed part of the electric circuit and provided filler to the weld joint. Wire was fed to the arc by an automatic wire feeder.

The welding was carried out with power source biased towards DC-electrode positive (DC-EP), this ensures electrons are accelerated from negative work piece onto the positive electrode with sufficient energy to melt the filler wire (Messler, 2008). The schematic diagram of the weldment is shown in Figure 1.

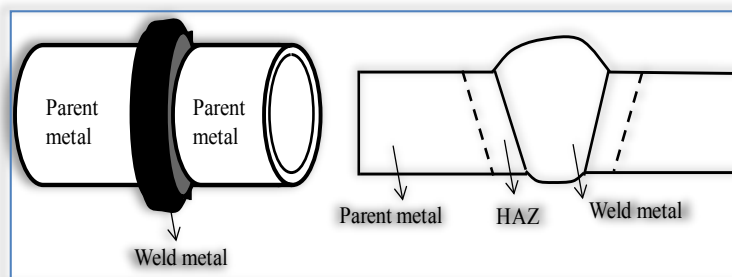


**Figure 1:** Schematic diagram of weldment showing parent metal, HAZ and weld metal

### 2.3. Optical Metallography of As-Weld Sample

Transverse section of as-welded specimen of dimensions 17×16×5 mm was sectioned from the welded girth ring. The specimen was mounted in bakelite powder on a METASERV automatic hot mounting press for easy handling. The sample was subsequently grinded with abrasive paper in order: 400, 600, 800, 1200 and 4000 grit sizes. Grinding operation was followed by mechanical polishing with 0.25  $\mu$ m diamond paste. Each successive stage of grinding and polishing was followed by washing and drying to avoid contamination.

The specimen was etched by immersion in picral for 3 minutes to reveal microstructures in the specimen. The concentration of picral used contained 5 g of picric acid and 2.5 ml HCl in 100 ml ethanol. The etched specimen was rinsed in water and later in ethanol before it was dried with warm air. The specimen was viewed under optical microscope at low magnifications. The different phases in the parent metal, the HAZ and weld metal were examined.

### 2.4. Four Point Bend Test in Sweet and Sour Environments

Transverse section of as-welded specimen of dimensions 100×15×3 mm<sup>3</sup> was sectioned from the welded girth ring with root surface left intact. The samples had been subjected to four point bend test (4PBT) during which the specimens was stressed to about 100% of the measured 0.2% yield strength in bolt-loaded jigs, to provide the necessary strain in the weldment toe and HAZ areas. Strain gauges had been used on the rear compression side of the weldment to measure the level of the strain during the tests (Woollin et al., 1999). The specimens were tested in deoxygenated brine for Stress Corrosion Cracking (SCC) in sour environment and sweet environment. The environmental variables of significance in the test were temperature and the presence of hydrogen sulphide and carbondioxide, the basis on which the environments were characterised

as sour and sweet respectively. The test condition also featured sodium hydrogen trioxocarbonate, ( $\text{NaHCO}_3$ ) which was used as a buffer to adjust the pH level. The welding processes, the 4PBT and the corrosion tests were all carried out at TWI, Cambridge.

**Table 2:** The corrosion test conditions used on the 4PBT specimens

Specimen	Temperature (°C)	PP*CO <sub>2</sub> (bar)	PP H <sub>2</sub> S (bar)	NaCl (%)	NaHCO <sub>3</sub> (ppm†)	pH	Environment
W2AXII	25	1	0.04	25	500	4.5	Sour
W2AVII	110	10	0	25	0	3.3	Sweet

\* Partial Pressure of gaseous molecules, † concentration in part per million

### 2.5. Scanning Electron Microscopy and Electron Backscatter Diffraction

The 4PBT specimen was prepared for scanning electron microscope (SEM) and EBSD by following the basic metallography sample preparation detailed in section 2.3. The specimen was subsequently polished with oxide polishing solution (OPS) for two hours on a polishing machine at the speed of 150 rev/min. The second round of polishing with OPS was necessary to help remove the surface strain introduced by previous mechanical grinding and polishing. JEOL SEM and CAMSCAN field emission gun scanning electron microscope (FEGSEM) were used for imaging and EBSD mapping on the specimen respectively. The EBSD provided additional information including grain disorientation and for the evaluation of the grain size across the weldment. The SEM was operated at accelerating voltage of 20 keV and the scanning step size of 0.5  $\mu\text{m}$  was used. The details on EBSD technique is fully described by Ahmed *et al.* (2014b).

Raw data obtained from Channel-five acquisition software were processed with VMAP software. The data were about 70% indexed and were cleaned to level 3 to amend the non indexed points. High angle boundary definition of greater than 15° was used, while grains with disorientation less than 15° were considered to be low angle boundary. These boundaries conditions have been adjudged the most widely used boundary definition (Humphreys, 2001).

## 3. RESULTS AND DISCUSSION

### 3.1. Metallographic Examination of As-weld Sample

The result of optical metallography of the weldment etched in picral is shown in Figure 2. The two obvious phases observed in the micrograph were martensite and ferrite phases. Retained austenite was not observed in the weldment. On the right hand side (RHS) of the micrograph was the parent material. The parent material contained equiaxed grains of martensite. The parent material was predominated with martensite with little amount of ferrite in the structure. The left hand side (LHS) of the micrograph in Figure 2 showed the weld metal. The plan nature of the weld metal was attributed to the higher corrosion resistance of weld metal. This result is consistent with the expectation because of the relatively higher corrosion (etchant) resistant superduplex stainless steel filler used for the fabrication. The HAZ covered about 50  $\mu\text{m}$  region between the parent (RHS) and weld (LHS) metals. This is shown in the middle of the micrograph in Figure 2. The HAZ have experienced grain growth with relatively larger grain sizes. The HAZ was dominated by large martensite plates.

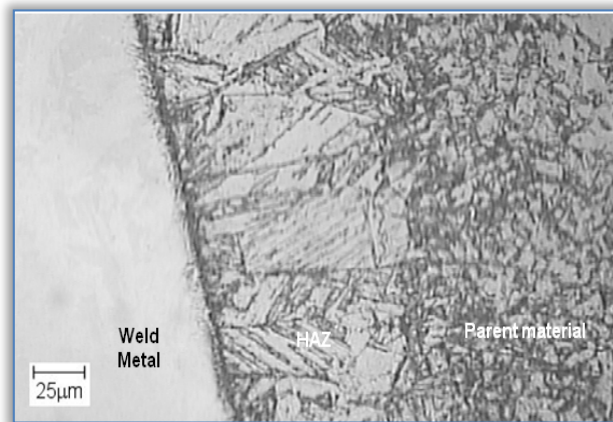


**Figure 2:** The Optical Micrograph of As-Welded Specimen Etched with Picral. The Micrograph Showed the Parent Material the HAZ and the Weld Metal

### 3.2. SEM and EBSD Micrographs of 4PB Specimen Tested in Sour Environment

The results of scanning electron microscopy and electron back scatter diffraction carried out on specimen W2AXII tested in sour environment are shown in Figure 3. Figure 3A shows the SEM image of the cracks tip and the EBSD map of the cracks tip is shown in Figure 3B.

In specimen W2AXII, the whole length of the crack occurred in the high temperature region of HAZ close to the fusion boundary. The crack path was initially close to the fusion boundary but the tip of the crack deflected towards the middle of the HAZ as shown by arrow heads in the Figure 3B. It is equally evident from Figure 3B that the crack path cut across the grains in the

HAZ. It can therefore be suggested from EBSD micrograph that the crack in specimen W2AXII was transgranular crack. The crack was tracked with dotted line for easy visibility. The morphology of the cracks in W2AXII tested in sour environment was predominantly transgranular in nature.

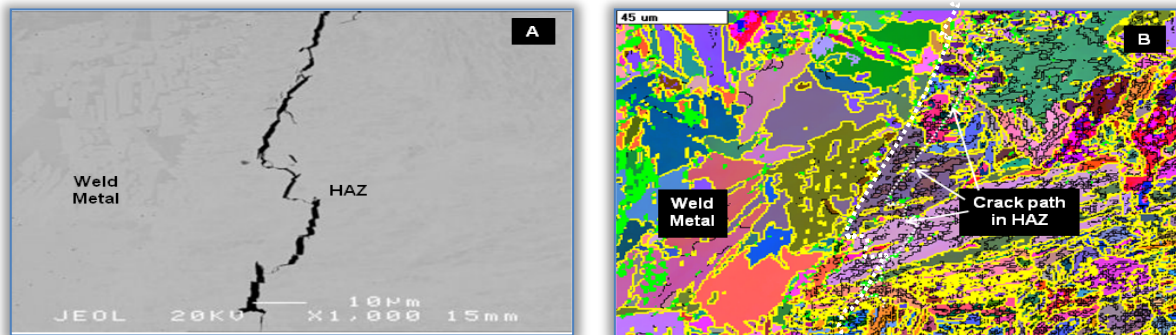


**Figure 3:** SEM Micrograph and EBSD Map of Specimen W2AXII Tested in Sour Environment Containing

Containing 1 bar CO<sub>2</sub>, 0.04 bar H<sub>2</sub>S, 25% NaCl, 500 ppm NaHCO<sub>3</sub>, pH of 4.5 and Temperature of 25°C

It is reasonable to link the observed cracks in the specimen with concentration of corrosion species in the environment, while the severity of the crack is not unconnected with acidity which is a function of pH level in the testing environment. Specimens W2AXII was exposed to environment containing hydrogen sulphide (H<sub>2</sub>S) partial pressures of 0.04 bar (see Table 2). The likely chemical reaction due to the presence of H<sub>2</sub>S in the environment is contained in Equation 1. The results indicated the possibility of reaction between the steel and H<sub>2</sub>S in the presence of water. The atomic hydrogen which occurred as a reaction product may diffuse into the lattice point, particularly the interstitial site and combined to form gas molecule. The presence of atomic hydrogen and hydrogen gas in interstitial site and areas of imperfection may render the material susceptible to SSC by hydrogen embrittlement (Gerus, 1974).



On the other hands, the super duplex stainless steel filler used to join the material during fabrication contained relatively higher amount of C and N. the higher concentration of these elements in the weld metal may promote diffusion across the narrow fusion boundaries into the high temperature HAZ (Woollin, 2007). C and N are known to have strong influence of the hardness properties of the martensites in the HAZ. From the result of hardness test of the as-welded specimen, the suggestion that cracks in sour specimens occurred by the mechanism of SSC is supported by the peak hardness value of 349HV10 which clearly surpassed the limit of 240HV10 (23HRC) specified by NACE (MR0175) for prevention of SSC of MSS in sour environment. It is important to mention that high hardness is an indication of high yield stress in the HAZ. The stress in the HAZ constitutes a driving force for SSC/SCC.

In addition to cracks, specimens W2AXII also showed pitting corrosion sites in the parent material. It is well established that, the presence of chlorides in test environment makes the sample more susceptible to formation and growth of pit (Sedriks, 1996). Table 2 shows that W2AXII was tested in sour environment containing 25% NaCl. In contrast, specimen W2AVII which was also subjected to NaCl sweet environment did not show any sign of pitting neither in the parent material nor in the HAZ.

### 3.3. SEM and EBSD Micrographs of 4PB Specimen Tested in Sweet Environment

The results of scanning electron microscopy and electron back scatter diffraction carried out on specimen W2AVII tested in sweet environment are shown in Figure 4. Figure 4A shows the SEM image of the cracks tip and the EBSD map of the cracks tip is shown in Figure 4B. The cracks initiated at the weld root and propagated in the HAZ within the neighbourhood of the fusion boundary with characteristic features of intergranular cracking. The cracks tip navigated across the HAZ along the grain boundaries into the parent material. The branches along the crack path and the crack tips (Figure 4) are overwhelming evidences of intergranular cracking. The size of the crack was relatively wider than those found in the sour specimens. This observation is consistent with the finding of Coudreuse *et al.* (1999).

The probable reasons for the severity of the crack in the W2AVII were the higher temperature and acidity of the testing environment. High temperature increases the rate of formation of carbonic acid (Equation 2) Therefore increasing the acidity of the local environment.



The presence of carbonic acid lowers the pH of the water in the system and it provides hydrogen ion as electron acceptors. The reduction in pH or the amount of carbonic acid is depended primarily upon the pressure at which the system is been operated. The rate of corrosion increases with increase in partial pressure of  $\text{CO}_2$ . But, the presence of some dissolved minerals in the environment may act as buffering agent to subjugate the reduction of pH level in the system (Gerus B. R. D., 1981). The formation of carbonic acid is a very slow process and the corrosion rate is expected to be slow at room temperature. But at elevated temperature, the severity of corrosion in  $\text{CO}_2$  environment increases with rise in temperature.

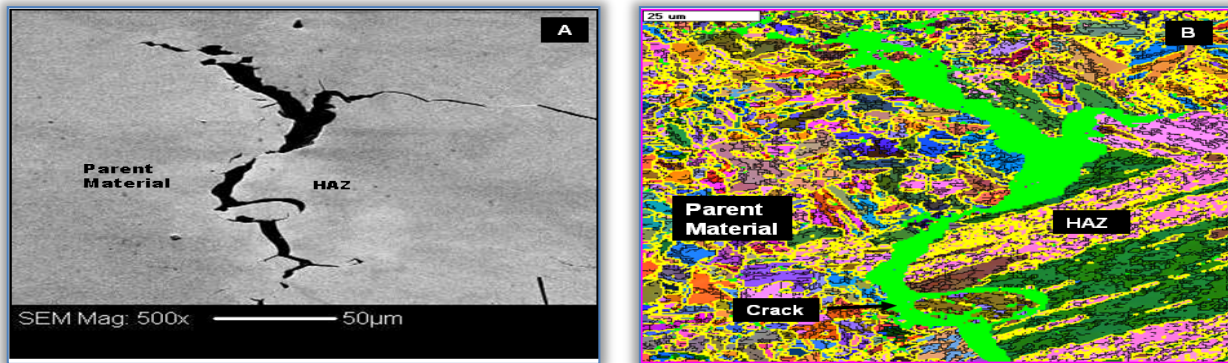


**Figure 4:** SEM Micrograph and EBSD Map of Specimen W2AVII Tested in Sweet Environment Containing 10 bar  $\text{CO}_2$ , 25% NaCl, 0 bar  $\text{H}_2\text{S}$ , 0 ppm  $\text{NaHCO}_3$ , pH of 3.3 and Temperature of  $110^\circ\text{C}$

The occurrence of intergranular cracks in specimen W2AVII is consistent with the mechanism of sensitization. Sensitization occurred as a result of precipitation Cr carbides preferentially along the prior austenite grain boundaries and in effect, leading to depletion of Cr content to the level below the requirement for corrosion resistance of the steel (Turnbull and Griffiths, 2003, Woollin, 2007, Woollin and Carrouge, 2002). The presence of carbides on the grain boundaries with a resultant low level of Cr within the immediate vicinity of the precipitates may make the grain boundaries to be anodic to its surrounding. Eventually, micro-galvanic corrosion may occur as a result of this process and the material becomes more susceptible to intergranular stress corrosion. On the other hand, the high density of C and N in the weld metal as a result of super duplex stainless steel filler may allow diffusion of these elements across the fusion boundaries into the high temperature HAZ. The C and N enrichment may be another justification for sensitization in the neighbourhood of fusion boundary region where the crack propagation was more dominant. These explain the reason for the occurrence of intergranular cracking in specimen W2AVII. Although considering the test temperature of  $110^\circ\text{C}$ , transgranular cracking is least expected in the specimen. However, the possibility of a ductile bridge cannot be overruled because of the higher temperature. The suggestion of ductile bridge is evident from the morphology of the crack in Figure 4 which showed an 'O' ring along the crack path in the HAZ.

On the other hand, the branches along the main crack and the tip of the cracks (Figure 4B) propagated along the prior austenite grain boundaries in the HAZ and in the parent material. It is supposed that disorientation between grains will have significant effect on intergranular crack growth. Disorientation is the minimum angle through which adjacent grain must be rotated to align it with its neighbour (Humphreys, 2001). If that be the case, one may expect easy crack growth in the region with low disorientation and vice versa. The disorientation in the HAZ is relatively lower than in the parent material. And, weld metal has almost double the disorientation in the HAZ. Most of the intergranular cracks occurred in the HAZ on both sides of the weld rather than the parent material. There was no crack in the weld metal.

#### 4. CONCLUSIONS

The following are the conclusions made at the end of the assessment of crack propagation mode in martensitic stainless steel HAZ, carried out with SEM and Electron Back Scatter Diffraction and with focus on the effects of environmental variables:

1. Metallographic examination of martensitic stainless steels revealed the classical regions of the weldment namely: the parent material; the heat affected zone; the weld metal.
2. The parent material was predominately equiaxed grains of martensite and the heat affected zone contained coarse martensite platelets.

3. The cracks in four-point bend specimens tested in sour environments containing H<sub>2</sub>S failed by sulphide stress corrosion cracking. The cracks were transgranular in nature. Sulphide stress corrosion cracking is likely to have occurred as a result of infiltration of atomic hydrogen into the interstitial sites with the formation of H<sub>2</sub> at crystallographic imperfections within the material.
4. The specimen tested in a sweet environment showed cracks which are dominated by intergranular features. The mechanism of intergranular stress corrosion cracking is consistent with intergranular carbide precipitation by sensitisation process in the heat affected zone.
5. Carbon enrichment of the heat affected zone closest to the weld metal may increase the propensity for chromium carbide precipitation at grain boundaries and hence increased susceptibility to intergranular stress corrosion cracking.
6. The heat affected zone had the lowest grain misorientation compared with parent and weld metals. Consequently, most of the intergranular cracks occurred in the HAZ on both sides of the weld metal rather than the parent metal.

**Acknowledgement:** The authors sincerely acknowledge the provision of specimens used for this project and technical supports by The Welding Institute (TWI), Cambridge, United Kingdom. Special thanks to Dr. Paul Woollin, Ms Sophia Necib and all staffs of TWI for their supports. The discussion and contribution of Professor Stuart Lyon is also acknowledged.

### References

- [1.] Ahmed, I. I., Grant, B., Sherry, A. H. & Quinta Da Fonseca, J.: Deformation path effects on the internal stress development in cold worked austenitic steel deformed in tension, *Materials Science and Engineering: A*, 614 (0), 326-337, 2014a.
- [2.] Ahmed, I. I., Wright, D., Adebisi, J. A., Aremu, I. N., Yahaya, T. & Quita Da Fonseca, J.: Assessment of Deformation Twinning in Cold Rolled Austenitic Stainless Steels with Electron Back Scatter Diffraction, *Nigerian Journal of Technological Development*, 11 (1), 7-11, 2014b.
- [3.] Aquino, J. M., Della Rovere, C. A. & Kuri, S. E.: Intergranular corrosion susceptibility in supermartensitic stainless steel weldments, *Corrosion Science*, 51 (10), 2316-2323, 2009.
- [4.] Coudreuse, L., Verneau, M. & Dufrane, J.: Sulphide stress cracking resistance of weldable supermartensitic stainless steels. *Proc. Supermartensitic Stainless Steels Brussel*. Belgian Welding Institute, 299-306, 1999.
- [5.] Enerhaug, J. & Steinsmo, U.: Factors affecting initiation of pitting corrosion in super martensitic stainless steel weldments, *Science and Technology of Welding & Joining*, 6 (5), 330-338, 2001.
- [6.] Gerus, B.: Detection and mitigation of weight loss corrosion in sour gas gathering systems. *SPE Symposium on Sour Gas and Crude*. Society of Petroleum Engineers, 1974.
- [7.] Gerus B. R. D.: Detection and Mitigation of Weight Loss Corrosion in Sour Gas Gathering Systems, In: Tuttle (Bob) R. N. & Kane (Russ) R. D., eds. *H<sub>2</sub>S Corrosion in Oil and Gas Production: A compilation of Classic Papers*, Houston, Texas. NACE, 1981.
- [8.] Griffiths, A., Nimmo, W., Roebuck, B., Hinds, G. & Turnbull, A.: A novel approach to characterising the mechanical properties of supermartensitic 13 Cr stainless steel welds, *Materials Science and Engineering: A*, 384 (1-2), 83-91, 2004.
- [9.] Hanneman, R. E., Rao, P. & Danko, J. C.: Intergranular Stress Corrosion Cracking in 304 SS BWR Pipe Welds in High Temperature Aqueous Environments. *Environment-Sensitive Fracture of Engineering Materials*, Chicago, Illinois. 153-177, 1979.
- [10.] Humphreys, F.: Review grain and subgrain characterisation by electron backscatter diffraction, *Journal of materials science*, 36 (16), 3833-3854, 2001.
- [11.] Kurahashi, H., Kurisu, T., Sone, Y., Wada, K. & Nakai, Y.: Stress Corrosion Cracking of 13Cr Steels in CO<sub>2</sub>-H<sub>2</sub>S-Cl-Environments, *Corrosion*, 41 (4), 211-219, 1985.
- [12.] Messler, R. W.: *Principles of welding: processes, physics, chemistry, and metallurgy*, John Wiley & Sons, 2008
- [13.] National Energy Board: Report of Public Inquiry Concerning Stress Corrosion on Canadian Oil and Gas Pipeline Steels. Report of NEB, MH. Canada, 1996.
- [14.] Sedriks, A. J.: *Corrosion of stainless steel*, John Wiley and Sons, Inc., New York, NY (United States), 1996
- [15.] Turnbull, A. & Griffiths, A.: Review: Corrosion and cracking of weldable 13 wt-% Cr martensitic stainless steels for application in the oil and gas industry, *Corrosion engineering, science and technology*, 38 (1), 21-50, 2003.
- [16.] Williams, D., Pao, P. & Wei, R.: The combined influence of chemical, metallurgical and mechanical factors on environment assisted cracking, 1979.
- [17.] Woollin, P.: Postweld heat treatment to avoid intergranular stress corrosion cracking of supermartensitic stainless steels, *Welding in the World*, 51 (9-10), 31-40, 2007.
- [18.] Woollin, P. & Carrouge, D.: Heat affected zone microstructures in supermartensitic stainless steels. *Conference on Super martensitic Stainless Steels*, Bruxelles, Belgique. 2002.
- [19.] Woollin, P., Noble, D. N. & Lian, B.: Weldable 13%Cr martensitic steels for pipeline applications: preliminary studies, *EPRG/PRCI 12th biennial joint technical meeting on pipeline research*. 1999.